

New Model for Reconstructed Si(111) 7×7 Surface Superlattices

J. C. Phillips

Bell Laboratories, Murray Hill, New Jersey 07974

(Received 21 May 1980)

Superlattices of disjoint bilayer atomic microdomains stabilized by epitaxial misfit strain energies are proposed to account for $n \times n$ ($n=5$ at lower T , $n=7$ at higher T) surface structures of *both* Si on Si(111) and Sn on Ge(111). The microdomain model accounts well for the relative stability of Si(111) 7×7 against hydrogenation and chlorination and is energetically more favorable than the original Lander model of 2×2 building blocks centered on point vacancies.

PACS numbers: 68.20.+t, 61.14.Hg, 68.10.Jy, 68.55.+b

A wide variety of superlattice patterns has been observed on almost every face of each predominantly covalent semiconductor which has been studied by low-energy electron diffraction.^{1,2} The largest $n \times n$ unit cells are found¹ on annealed Si(111) surfaces: For the pure surface, $n=7$ (annealed at $T_a > 600$ C), or $n=5$ ($T_a < 600$ C). Recently it has been discovered³ that a fraction of a monolayer of Sn on Ge(111) unexpectedly converts the annealed 2×8 Ge superlattice to a Si-like pattern ($n=5$, $T_a < 400$ C; $n=7$, $T_a > 400$ C). In this note, I propose a new theoretical model which explains the remarkable similarity in the thermal behavior of these giant $n \times n$ cells and which also reconciles a wide range of paradoxical data. These include the dependence⁴ of the annealing temperature T_c for converting cleaved Si 2×1 to 7×7 on regular macroscopic step density [vicinal (111) surfaces] and the relative stability of Si(111) 7×7 (unlike cleaved 2×1) against hydrogenation⁵ and chlorination.⁶

Broadly speaking the theoretical models which have been suggested^{7,8} to explain reconstructed superlattice structures on predominantly covalent semiconductor surfaces are divided into two types, rough and smooth. The smooth models assume that the surface is atomically complete (apart from a small density of random macroscopic steps) and that the observed low-energy electron-diffraction (LEED) superlattice patterns are produced by small periodic displacements ($\delta b/b \approx 0.1$) of atoms in the surface plane from the sites of a semi-infinite bulk lattice. The forces responsible for the weak reconstruction are of the Jahn-Teller type and may be electronic density waves (of the Peierls-Overhauser type) which are formed because of the specific geometry of the Fermi line of the dangling-bond surface electronic energy band,⁹ or, more generally,¹⁰ by the interatomic forces responsible for the buckling of the cleaved Si(111) 2×1 surface.

The present rough model assumes that because of the kinetics of surface preparation (which, in one way or another, are at best equivalent to thermal roughening of the surface, as in high-temperature annealing, or at worst produce a grossly damaged surface, as in a "poor" cleave) the surface will always be incomplete or fragmented on an atomic scale.¹¹ This means that over the surface area of order 10^2 surface sites required to define the observed LEED pattern about 50 (± 10) excess surface atoms will be distributed. What becomes of these excess atoms during the initial stages of annealing? The answer, of course, is that the excess surface atoms condense to form $m \times m$ islands ($m < n$). These islands will be nearly maximally compact, i.e., their shape will nearly maximize their area/circumference ratio. For (111) surfaces this means that the islands will be nearly hexagonal and will be bounded by linear edges composed of (110) steps.⁷ The same kinetics describe the later stages of annealing³ of a fraction (0.3–0.8) of a monolayer of Sn on Ge(111).

At this point we can already make a fundamental distinction between the rough atomic and smooth displacive models based on the energy ΔE_s available for superlattice ordering. The smooth models yield values of ΔE_s which range from very small ($\Delta E_s^p \approx 0.005$ eV/atom) for the Peierls mechanism¹² to small ($\Delta E_s^b \approx 0.02$ eV/atom) for the buckling model.¹⁰ The rough values lead to a much larger value for ΔE_s ⁷ because of the nonlocal or cumulative nature of the misfit strain energy associated with epitaxial film interfaces,¹³ which is illustrated for Sn on Ge in Fig. 1(a).

While the application of epitaxial strain arguments to the strong reconstruction of fractional monolayers of Sn on Ge is obvious, it is somewhat less obvious for Si on Si. In fact the latter case is special, because the fractional surface

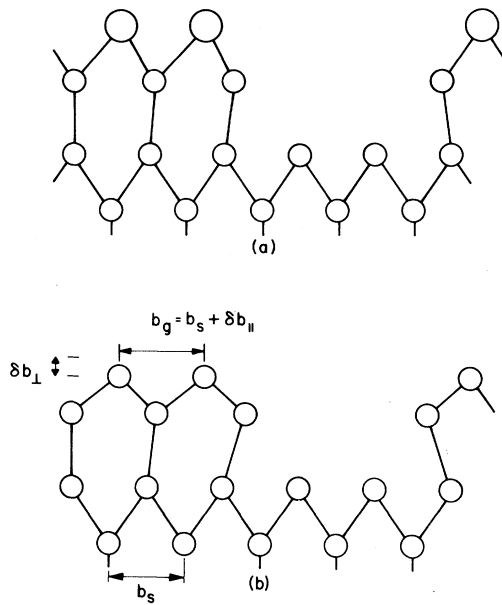


FIG. 1. (a) A cross section of part of an $n=5$ and $m=4$ Sn microdomain on Ge(111), but not to scale [$r(\text{Sn}) = 1.15r(\text{Ge})$]. Some of the sites in the troughs between Sn-covered islands may be occupied by Ge atoms (as superlattice defects) and some of the Sn atoms may similarly replace Ge in second-layer sites. (b) The same for Si on Si(111). The distortions of the upper layers are exaggerated. Strong reconstruction which is significantly resistant to chemical corrosion results when these microdomains order to form superlattices.

layers on Si(111) are almost certainly fractional bilayers, so that there is only one broken bond per surface atom [except for the (110) steps which define the microdomain edges]. These bilayers are compressed by inward relaxation¹⁴ of the outer atomic layer (enhanced back bonding). Unlike C, Si does not readily form multiple bonds, and the inward vertical relaxation δb_{\perp} may produce a lateral expansion δb_{\parallel} , i.e., the effective lattice constant b_g of the fractional surface bilayer may be larger by δb_{\parallel} than that, b_s , of the substrate, as shown in Fig. 1(b). However, we are justified in treating δb_{\perp} and δb_{\parallel} as symmetry-breaking constants (c numbers, in the language of field theory) only so long as the strain energy $k(m\delta b_{\parallel})^2$ is $\lesssim \Delta E_R$, where ΔE_R is the relaxation energy of the cleaved surface. (We expect that ΔE_R is of order the step-formation energy ΔE_{SF} and from the shifts of dangling bond energies with surface relaxation¹⁴ that both energies are of order 0.3 eV/atom.) Subject to this condition the size-limiting energetics of microdomain growth of Si on Si(111) may resemble those of Sn on

Ge(111). The very striking quantitative similarities in $n(T_a)$ are discussed below.

The mechanism of epitaxial, microdomain, strain misfit energies immediately can explain the paradox that for both Sn on Ge(111) and Si bilayers on Si(111) the $n=5$ superlattice is stable at lower temperatures, contrary to bulk structural transitions where according to Ostwald's rule generally the smaller unit cell is stable at higher temperatures. (No other model which has been proposed can explain this anomaly.) The surface interatomic force constants, because of reduced atomic coordination numbers and lower surface phonon frequencies, soften more rapidly at high temperatures than the bulk force constants. Hence the nonlocal misfit strain energy (which limits m and n) decreases more rapidly than the local rebonding energies associated with step formation (which tend to increase m and n) with increasing T , which explains why the larger value of n is stable at higher T .

In principle as the temperature is increased and the surface force constants soften further, an entire sequence of additional transitions to still larger microdomain structures (e.g., $n=9$, etc.) could occur. However, at high temperatures the edges (steps) of the microdomains will also undergo thermal roughening.¹¹ Recent LEED experiments have shown¹⁵ that an order-disorder transition of the 7×7 structure occurs at $T_c = 854^\circ\text{C}$ with small but discernible kinetic hysteresis. Evidently such a transition (essentially a transition to a roughened surface) can preclude additional transitions to larger values of n . Moreover microdomain edge roughening (rather than mere center positional disordering) can explain the rather puzzling absence of long-wavelength critical scattering¹⁵ as T approaches T_c , because the characteristic wavelength of edge roughening is the diameter of the 7×7 cell itself.

The steps associated with microdomain edges will tend to be pinned by extended (macroscopic) steps, e.g., produced by a vicinal cleave, and the temperature T_c for conversion of the cleaved surface to the microdomain surface will depend strongly on the macroscopic step density.⁴ When that density is very low T_c may be as low as 200 C, and this observation has often been used as an objection against rough models.¹⁰ Note, however, that if, as we suppose, the roughness is of thermal origin and hence is intrinsic, the average atom during annealing need diffuse a distance d which is only $d \approx (n-m)b < 10 \text{ \AA}$, and that this could easily happen at 200 C. (Evaporated Si

atoms diffuse 40 Å during island growth of amorphous Si on substrates at He temperatures.¹⁶⁾

The stability of the $n=7$ Si(111) pattern against hydrogenation⁵ and chlorination⁶ (which remove the dangling bonds and erase both the Fermi line and the surface buckling) is a very sore point for smooth models. This chemisorption also erases most of the difference δb_{\perp} between b_g and b_s . However, because of the large number of overlaid atoms in a given bilayer microdomain, these units will be collectively metastable for much longer periods¹⁷ than a simple Jahn-Teller local distortion and will resist chemical attack to a much greater degree than would hold for the smooth models.

What about the remarkable similarity of $n(T_a)$ for Si bilayers on Si and Sn on Ge? This is probably largely coincidental, and may occur because $k(\text{Si on Si})(b_g - b_s)^2$ is of the same order as $k(\text{Sn on Ge})(b_{\text{Sn}} - b_{\text{Ge}})^2$. Here the k 's represent interatomic forces, and $k(\text{Si on Si}) > k(\text{Sn on Ge})$, while $(b_g - b_s)^2 < (b_{\text{Sn}} - b_{\text{Ge}})^2$. The actual values of $m(n)$ are determined by kinetic constraints and by strain-misfit and step-step interaction energies which taken altogether are quite complex. However, it is tempting to suppose that $m = n - 1$, because, as pointed out by Kane,¹⁸ when m is even the bilayer hexagonal corners are rounded in the upper monolayer in an energetically favorable way.

A useful distinction can be made between nearly hexagonal superlattice overlaid bilayers and the isolated triangular growth pyramids which have been observed¹⁹ to nucleate homogeneously on Si(111) surfaces during vapor deposition. The former situation, obtained by annealing a rough surface, resembles a two-dimensional liquid-solid transition. Coalescence of the microhexagons is forbidden by the accumulation of strain misfit energy. In the latter case multiple bilayers grow from the vapor, and the upper layers erase the strain energy of the layers below them, which gives rise to a triangular morphology because of the inequivalence⁷ of (110) and $(\bar{1}\bar{1}0)$ macroscopic step energies.

The present model of misfit-stabilized superlattices apparently is not appropriate to superlattice patterns of low symmetry such as noncompact Ge(111) 2×8 . Although this surface must also be atomically rough, general thermodynamic arguments show²⁰ that the covalency in Ge (taking as a fiducial point Sn, which is found in both covalent and metallic forms) is about $\frac{2}{3}$ as great as in Si. It is therefore possible that annealing

of Ge(111) surfaces produces some regions which are atomically smooth and which are weakly reconstructed. This would be consistent with the partial erasure of the Ge(111) 2×8 structure by hydrogenation.⁶

In conclusion, the more intuitively favored models for annealed and reconstructed semiconductor surfaces, and especially natural cleavage faces such as Si(111) and Ge(111), are essentially smooth and atomically complete. I have argued, however, that the weight of recent experimental evidence favors entirely new and much less obvious microfaceted models containing superlattices of islands, troughs, and steps. The hidden mechanism which favors these surprising structures is a large epitaxial strain misfit energy which is probably present even on pure surfaces. If the present model is correct it has far reaching implications, e.g., it can explain the otherwise puzzling absence of critical scattering at the superlattice disordering transition,¹⁵ and it should have important consequences for the interpretation of some semiconductor heterointerface experiments as well.²¹ More quantitative characterization of the microfaceted dimensions within a unit cell requires a detailed analysis of atom diffraction data.^{22, 23}

I am grateful to M. J. Cardillo and J. E. Rowe for helpful discussions.

¹J. J. Lander, in *Progress in Solid State Chemistry*, edited by H. Reiss (Pergamon, Oxford, 1965), Vol. 2, p. 26. Lander was able to observe $n=5$ only "by prolonged annealing" below T_a .

²F. Jona, IBM J. Res. Dev. **9**, 357 (1965). Jona, working with cleaner surfaces than Lander, did not observe $n=5$. He concluded that Lander's surfaces contained impurities which "favored" $n=5$ below T_a . I would prefer to say that impurities (such as Ni) were present on Lander's surfaces which *catalyzed* the otherwise sluggish formation of $n=5$ superlattices for T below T_a . See also E. Bauer, *Vacuum* **22**, 539 (1972), who reports that Fe [(Ni)] has a "beneficial" [read catalytic] effect in producing the 7×7 [(5×5)] structure in some experiments. The Fe(Ni) chemical specificity here may be primarily thermal rather than structural, i.e., it may simply reflect the relative lowest eutectic temperatures T_e of Fe-Si (1200 °C) and Ni-Si (960 °C) as given by M. Hansen, *Constitution of Binary Alloys* (McGraw-Hill, New York, 1958). See also G. Ottaviani, K. N. Tu, and J. W. Mayer, *Phys. Rev. Lett.* **44**, 284 (1980).

³T. Ichikawa and S. Ino, *Solid State Commun.* **27**, 483 (1978). Note that even low-melting-point Sn films exhibit sluggish hysteretic effects in transforming from $n=7$ to $n=5$ and back. It would be of interest to form $\text{Sn}_{1-x-y}\text{Pb}_x\text{Bi}_y$ submonolayer films on Ge and to study

the hysteresis of this transition as a function of x and y .

- ⁴P. P. Auer and W. Mönch, *Surf. Sci.* **80**, 45 (1979).
⁵K. C. Pandey, T. Sakurai, and H. D. Hagstrum, *Phys. Rev. B* **15**, 3648 (1977).
⁶T. Sakurai and H. D. Hagstrum, *Phys. Rev. B* **12**, 5349 (1975); J. E. Rowe, *Surf. Sci.* **53**, 461 (1975).
⁷J. C. Phillips, in *Physics of Semiconductors*, edited by F. G. Fumi (Tipografia Marves, Rome, 1976), p. 12.
⁸E. Tosatti, in *Physics of Semiconductors*, edited by F. G. Fumi (Tipografia Marves, Rome, 1976), p. 21.
⁹E. Tosatti and P. W. Anderson, *J. Appl. Phys. Jpn. Suppl.* **2**, 381 (1974).
¹⁰D. J. Chadi *et al.*, *Phys. Rev. Lett.* **44**, 799 (1980).
¹¹W. K. Burton, N. Cabrera, and F. C. Frank, *Philos. Trans. Roy. Soc. London, Ser. A* **243**, 299 (1951).
¹²J. E. Rowe and J. C. Phillips, *Phys. Rev. Lett.* **32**, 1315 (1974).
¹³F. C. Frank and J. H. Van der Merwe, *Proc. Roy. Soc.* **198**, 205 (1949).
¹⁴J. A. Appelbaum and D. R. Hamann, *Phys. Rev. Lett.* **31**, 106 (1973); see also J. C. Phillips, *Surf. Sci.* **40**, 459 (1973), for another way of estimating ΔE_{SF} in terms of residual broken bond energies, which gives about the

same answer.

- ¹⁵P. A. Bennett and M. B. Webb, private communication.
¹⁶J. J. Hauser, *Phys. Rev. B* **8**, 3817 (1973).
¹⁷C. Herring and M. H. Nichols, *Rev. Mod. Phys.* **21**, 185 (1949); see especially the discussion of the relative importance of thermodynamic and kinetic factors in forming etch pits (which are the inverse of islands), p. 257 ff.
¹⁸E. O. Kane, private communication.
¹⁹M. Shimbo, J. Nishizawa, and T. Terasaki, *J. Cryst. Growth* **23**, 267 (1974).
²⁰See Phillips. Ref. 14.
²¹J. L. Shay, S. Wagner, and J. C. Phillips, *Appl. Phys. Lett.* **28**, 31 (1976).
²²M. J. Cardillo and G. E. Becker, *Phys. Rev. Lett.* **42**, 508 (1979).
²³Very recently S. Ino, *J. Appl. Phys. Jpn.* **19**, L61 (1980), has presented reflection high-energy electron-diffraction data for Si(111) 7×7 . It appears that these data do not have correct symmetry, as one can show by transforming the rhombic unit cell to an hexagonal unit cell.

Observation of Crossover in the Dynamic Exponent z in Fe and Ni

Lee Chow and Christoph Hohenemser

Department of Physics, Clark University, Worcester, Massachusetts 01610

and

Robert M. Suter

IBM T. J. Watson Research Laboratory, Yorktown Heights, New York 10598

(Received 4 March 1980)

Time-differential perturbed angular correlations have been determined with use of the dynamical critical exponent z for Fe and Ni. In both systems, crossover from $z = 2.5$ to $z = 2.0$ is observed as $T \rightarrow T_C$. The value $z = 2.5$ ($d = 3$ Heisenberg model) has been previously observed in neutron-scattering experiments; the value $z = 2.0$ (order-parameter-nonconserving models), in hyperfine-interaction experiments. Thus, the existence of two distinct kinds of dynamic critical behavior, each corresponding to a different universality subclass, is confirmed.

PACS numbers: 64.60.Ht, 75.50.Bb, 75.50.Cc, 76.80.+y

Spin fluctuations near the Curie temperature in ferromagnets have been studied via neutron scattering and hyperfine interaction methods. For the isotropic, three-dimensional systems Fe and Ni, neutron scattering yields dynamic exponent values of $z = 2.7(2)$ and $z = 2.46(25)$,^{1,2} respectively. In contrast, hyperfine-interaction studies invariably produce $z = 2.0(2)$ for the same materials.³⁻⁷

In a recent Letter,⁸ two of us addressed this apparent discrepancy by suggesting that the effective value of z crosses over from 2.5 to 2.0 as the wave vector of the contributing fluctuations becomes small. To justify our hypothesis, we

noted that neutron scattering experiments depend predominately on "large" values of q , while hyperfine experiments probe the region near $q = 0$.

From a theoretical point of view, the value $z = 2.5$ is expected for the three-dimensional Heisenberg model (a system that has a conserved order parameter), while $z \cong 2.0$ is predicted for systems that contain appreciable order-parameter-nonconserving terms.⁹ Our crossover hypothesis therefore demands identification of suitable spin-nonconserving perturbations, as well as, eventually, explicit calculation of crossover behavior.

From an experimental point of view, the best